An anatomical investigation of the suboccipital- and inferior suboccipital triangles

Kirsten Shannon Regan, Gerda Venter

Department of Anatomy, Faculty of Medicine, University of Pretoria, Pretoria, South Africa

Abstract: The suboccipital triangle (ST) is a clinically relevant landmark in the posterior aspect of the neck and is used to locate and mobilize the horizontal segment of the third part of the vertebral artery before it enters the cranium. Unfortunately, this space is not always a viable option for vertebral artery exposition, and consequently a novel triangle, the inferior suboccipital triangle (IST) has been defined. This alternative triangle will allow surgeons to locate the artery more proximally, where its course is more predictable. The purpose of this study was to better define the anatomy of both triangles by measuring their borders and calculating their areas. Ethical clearance was obtained from the University of Pretoria (reference number: 222/2021) and both triangles were subsequently dissected out on both the left and right sides of 33 formalin-fixed human adult cadavers. The borders of each triangle were measured using a digital calliper and the areas were calculated using Herons Formula. The average area of the ST is 969.82 ± 153.15 mm^2, while the average area of the IST is 307.48 ± 41.31 mm^2. No statistically significant differences in the findings were observed between the sides of the body, ancestry, or sex of the cadavers. Measurement and analysis of these triangles provided important anatomical information and speak to their clinical relevance as surgical landmarks with which to locate the vertebral artery. Of particular importance here is the IST, which allows for mobilisation of this artery more proximally, should the ST be occluded.

Key words: Cervical vertebrae, Inferior suboccipital triangle, Obliquus capitis inferior, Suboccipital triangle, Vertebral artery

Introduction

Located within the posterior region of the neck, is a clinically important anatomical triangle known as the suboccipital triangle (ST). This triangle is limited superiorly and medially by the rectus capitis posterior major (RCPM) muscle, superiorly and laterally by the obliquus capitis superior (OCS) muscle, and inferiorly and laterally by the obliquus capitis inferior (OCI) muscle [1-3]. Its contents include the horizontal segment of the third part (V3) of the vertebral artery (V3h),

the suboccipital venous plexus, and the suboccipital nerve (the dorsal ramus of the first cervical spinal nerve) [2, 4, 5].

Comprising the floor of the ST is the posterior atlantooccipital membrane and the posterior arch of the first cervical vertebra (C1, also known as the atlas). This atlantooccipital membrane can be found between the posteroinferior aspect of the occipital bone and foramen magnum, and the posterior arch of the C1 vertebra. Anterior to this membrane is the first cervical spinal nerve and its rami (the dorsal ramus becomes the suboccipital nerve, located in the ST), the periarterial autonomous nervous plexus, and the venous compartment [2, 6].

This venous compartment presents as a sinus-like structure known as the suboccipital cavernous sinus. This suboccipital cavernous sinus encloses and cushions the horizontal part of the third segment of the vertebral artery within the ST. This sinus continues inferiorly below the transverse fora-

Corresponding author:
Gerda Venter (ORCID)
Department of Anaotmy, Faculty of Medicine, University of Pretoria, Prinshof Campus, Pretoria 0001, Gauteng, South Africa
E-mail: gerda.venter@up.ac.za

men and gradually becomes the vertebral venous plexus that surrounds the vertical part of the third segment of the vertebral artery (V3v) [6].

This triangle is classically used as an anatomical landmark during surgical procedures within the suboccipital region, to identify the vertebral artery as it travels from the transverse foramen of the second cervical vertebra (C2, also known as the axis) to the transverse foramen of the C1 vertebra in a medial to lateral direction [5, 7]. Visualization of the vertebral artery within this triangle is sometimes challenging due to occlusion by scar tissue from previous surgical procedures, or anomalous anatomy, especially involving the vertebral artery [8-10]. Because the course and location of V3 exhibits such a large amount of variation in relation to the C1 and C2 vertebrae within ST, injury of this vertebral artery (and sometimes of the associated occipital nerves) is a potentially dangerous complication of many cranio-cervical procedures. Exposure and control of V3 proves to be significantly more challenging in the ST than at more proximal levels because of the arteries complex course [11]. Comprehensive knowledge of the anatomy of this artery is therefore vital when planning a surgical approach [12].

Identification of this artery (V3) and its surrounding structures are a key step in cranio-cervical procedures, including far lateral approach [13]. However, the intricate anatomy of this area, and the largely variable course and location of V3 within the ST make this visualization challenging. Therefore, exposition of V3 in this triangle is not always the most effective method of preventing iatrogenic vertebral artery injury.

To avoid potential injury to the vertebral artery in this region, an alternative, novel approach to locating this vessel at a more proximal location, was investigated. In this location, termed the "inferior suboccipital triangle (IST)" [9] - henceforth referred to as the IST - the vertical segment of the third part of the vertebral artery (V3v) can be exposed. As it runs from the transverse foramen of C2 vertebra to the transverse foramen of the C1 vertebra, which is situated in a slightly more lateral plane, it detaches itself from the lateral vertebral wall, making it more accessible. Additionally, the vertebral artery venous plexus that surrounds V3v is less significant at this lower level. No noteworthy looping or kinking of the artery was discovered within this triangle, and its course has been found to be significantly more predictable than its more distal aspects within the ST and above [9]. The borders of this novel triangle can be defined as the OCI muscle supe-

riorly, the posterior intertransversarii muscle inferiorly and laterally, and the lamina of the second cervical vertebra inferiorly and medially and are illustrated in Fig. 1. In this study, the superior border of the IST is specifically defined to be the length of the OCI from its insertion point on the transverse process of the C2 vertebra, to the point of intersection of its inferior border with the superior border of the lamina of C2.

This novel triangle holds great potential for the development of new and more effective methods of vertebral artery exposure during surgical procedures, when exposition via the ST is challenging or not possible [8]. To the author's knowledge, the study performed by La Rocca et al. [9] is the only piece of literature published on this novel inferior triangle, and the sample size of the study is small, consisting of only five cadavers.

The aim of this study was to examine and better understand the anatomy of this triangle as well as to produce more statistically significant data in a sample of adult human cadavers by measuring the length of the muscular and osseous structures forming the borders of both the ST and the IST and calculating the areas of both triangles. Additionally, the study aimed to compare the data obtained to any previously published studies regarding the size of the ST and IST. Lastly, the study sought to determine whether any correlation existed between the measurements taken and ancestry, sex or left and right sides of the body.
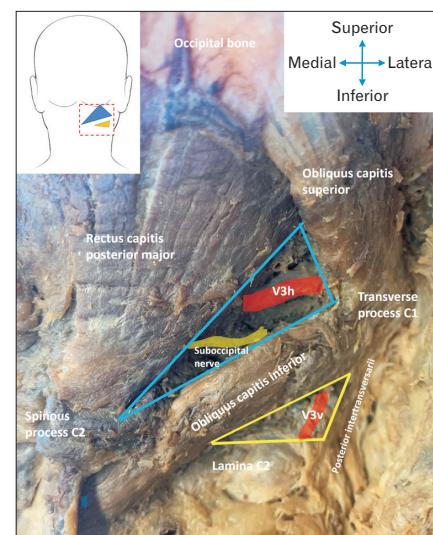

Fig. 1. Specimen image illustrating the borders of the ST (blue) and IST (yellow) triangle, indicating that the vertebral artery runs through both triangles. ST, suboccipital triangle; IST, inferior suboccipital triangle.

Materials and Methods

This study was a largely exploratory study with a descriptive, cross-sectional design. All the dissections for this study occurred in the dissection halls of the Department of Anatomy, Faculty of Health Sciences of the University of Pretoria, Pretoria, South Africa. This study's sample consisted of 33 formalin-fixed, human, adult cadavers with an age range of 18 to 96 years old. Of the sample, 22 cadavers were male, and 11 were female, while 28 belong to the white ancestry-group and five to the black ancestry-group. Each cadaver was dissected bilaterally within the suboccipital region to expose the ST and the IST on both the left and the right sides.

Only adult cadavers that have no anatomical abnormalities within the suboccipital region, as well as no previous surgical procedures within the posterior aspect of the neck were included in this study. Only cadavers in whom both the left and the right sides could be observed were included. Cadavers were not excluded based on age, race, or cause of death, unless the cause of death has resulted in the inaccessibility of the suboccipital region. If damage occurred to the region during the dissection process, that cadaver was potentially also excluded. This exclusion was entirely dependent on the degree of damage that occurred.

Procedure

The cadavers were placed in a prone position, skin incisions made, nuchal ligament cut and reflected, and the anatomical landmarks, as seen in Fig. 2, were exposed (dissection procedure adapted from Detton, 2017, p.9.) [14]. The visibility of the vertebral artery within the IST was defined by either a "yes" or a "no", and the areas of the triangles were calculated.

Measurements

Several landmarks were identified before the measurements of the muscles and related structures could be taken. These landmarks are summarised in Table 1 and visually represented in Fig. 2.

Once all the landmarks were identified, several measurements were taken (in mm) using a digital calliper. These measurements are summarized in Table 2 and illustrated in Fig. 3.

Once all relevant measurements were taken, the areas of the triangles (mm^2) were calculated using Herons Formula [15]. This formula was specifically chosen because it uses the length of all sides of the triangle, as well the value of the semi-perimeter of the triangle (rather than the traditional trigonometric method of using the values of relevant angles,

Table 1. A table representing the physical landmarks for measurements of both triangles' borders

Landmark	Description
A	Origin of RCPM muscle on C2 vertebral spinous process
B	Insertion of RCPM on occipital bone
C	Origin of OCS muscle on C1 vertebral transverse process
D	Insertion of OCS muscle on occipital bone
E	Origin of OCI muscle on C2 vertebral spinous process
F	Insertion of OCI muscle on C1 vertebral transverse process
G	Point of intersection between the inferior border of OCI and superior border of the lamina of C2 vertebra
H	Origin of posterior intertransversarii muscle between the transverse processes of C1 and C2 vertebrae
I	Insertion of posterior intertransversarii muscle between the transverse processes of C1 and C2 vertebrae
J	Start of the lamina of C2 vertebra as it relates to OCI
K	Termination of the lamina of C2 vertebra

RCPM, rectus capitis posterior major; OCS, obliquus capitis superior; OCI, obliquus capitis inferior.
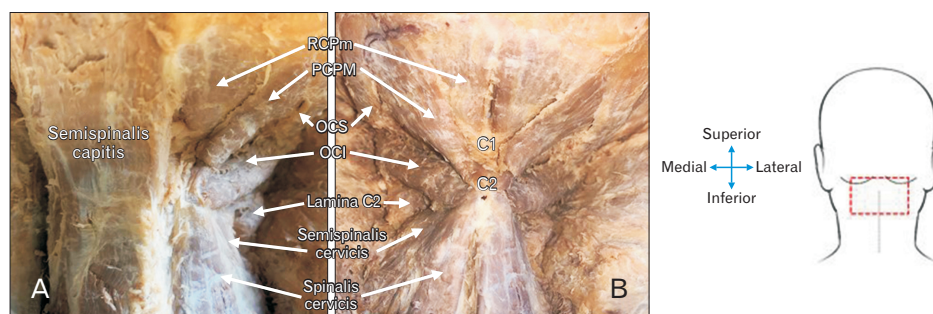

Fig. 2. (A) Image of exposed right suboccipital region with the right ST and IST and associated muscles visible, while the left semispinalis is still intact, covering the left ST and IST. (B) Image of trapezius, splenius capitis, semispinalis capitis muscles reflected to expose both the left and right suboccipital regions. ST, suboccipital triangle; IST, inferior suboccipital triangle; RCPm, rectus capitis posterior minor; RCPM, rectus capitis posterior major; OCS, obliquus capitis superior; OCI, obliquus capitis inferior.

Table 2. A table indicating the identification and description of measurements taken in this study

Measurement identifier	Description
AB	Length of RCPM muscle from origin to insertion
CD	Length of OCS muscle from origin to insertion
EF	Length of OCI muscle from origin to insertion
FG	Length of OCI muscle from the point of intersection between its inferior border and the superior border of the lamina of C2 vertebra, to its insertion
HI	Length of the posterior intertransversarii muscle as it runs between the transverse processes of C1 and C2 vertebrae
JK	Length of the lamina of C2 vertebra, from its start in relation to OCI, to its termination

RCPM, rectus capitis posterior major; OCS, obliquus capitis superior; OCI, obliquus capitis inferior.

Fig. 3. Image indicating the relevant measurements taken for both the ST (blue measurements) and the IST (yellow measurements). ST, suboccipital triangle; IST, inferior suboccipital triangle; RCPM, rectus capitis posterior major; OCS, obliquus capitis superior; OCI, obliquus capitis inferior; PI, posterior intertransversarii.

as no angles were measured in this study). The three lengths (borders of the ST and the IST), as used in Heron's formula were demarcated with 'a', 'b', and 'c', respectively.

'a' referred to the length of the RCPM in the ST and the length of the OCI in the IST (in mm).

'b' referred to the length of the OCS in the ST and the length of the posterior intertransversarii muscle, between C1 and C2 vertebrae, in the IST (in mm).

'c' referred to the length of the OCI in the ST and the length of the lamina of C2 vertebra in the IST (in mm).

All statistical analysis procedures were performed using IBM SPSS Statistics for Windows, version 22.0 (IBM Co.). This study focussed largely on descriptive statistics to illustrate the data obtained. Interferential statistical analysis included a Shapiro-Wilk test for data normality and paired sample t-tests to compare the measurements obtained on left and right sides. Furthermore, Pearson's chi-square tests were conducted to explore possible correlations between the measurements and the sex or ancestry of the cadaver. As well as intraclass correlation coefficient (ICC) tests to investigate the reliability of the measurements. All P-values of ≤0.05 were statistically significant. The sample size for the descriptive statistical analysis was 32 rather than the original 33 cadavers that were dissected. This is because one of the cadavers had a damaged right suboccipital region because of a previous dissection, and this cadaver was consequently excluded from this sample as it would have affected the data to have an unequal number of right and left measurements.

Ethical clearance was obtained from the Research Ethics Committee of the Faculty of Health Sciences of the University of Pretoria in May 2021 (reference number: 222/2021).
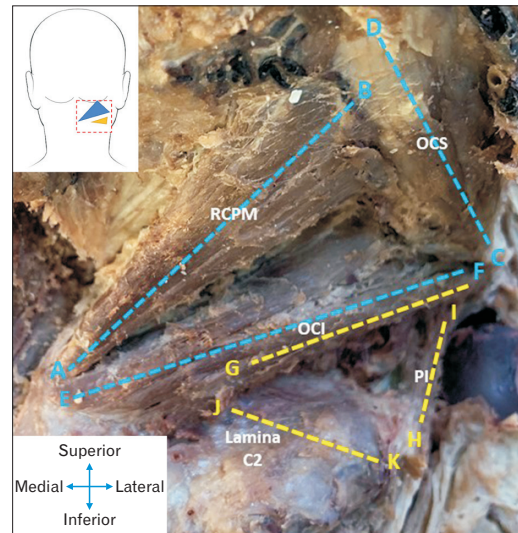
This clearance pertains to the conductance of a cadaveric study, that does not include any animals or living patients/volunteers, and the use of data collected from brain specimens. Cadaveric studies were conducted in accordance with the guidelines set by the National Health Act, 61 of 2003, as well as the 1964 Declaration of Helsinki and all subsequent revisions.

Results

Descriptive analysis of the data obtained by this study include the mean, minimum and maximum values, the range, and the standard deviation of each measurement on both the left and right suboccipital region, as well as the areas of the ST's and IST's on both sides. This data is summarised and illustrated in Fig. 4.

The area of the ST is very consistent, with the average areas equalling 970.1±0.79 mm^2 and 969.53±155 mm^2 for the right and left triangles, respectively and the difference between the average areas equalling less than 1 mm^2. The average areas of the IST's exhibit slight variation, with a difference of approximately 6 mm^2 between the average area of the right triangle (310.84±42.08 mm^2) and the left triangle (306.68±40.55 mm^2). This variation is minimal, and it can therefore still be said that the areas of the IST's are also con-
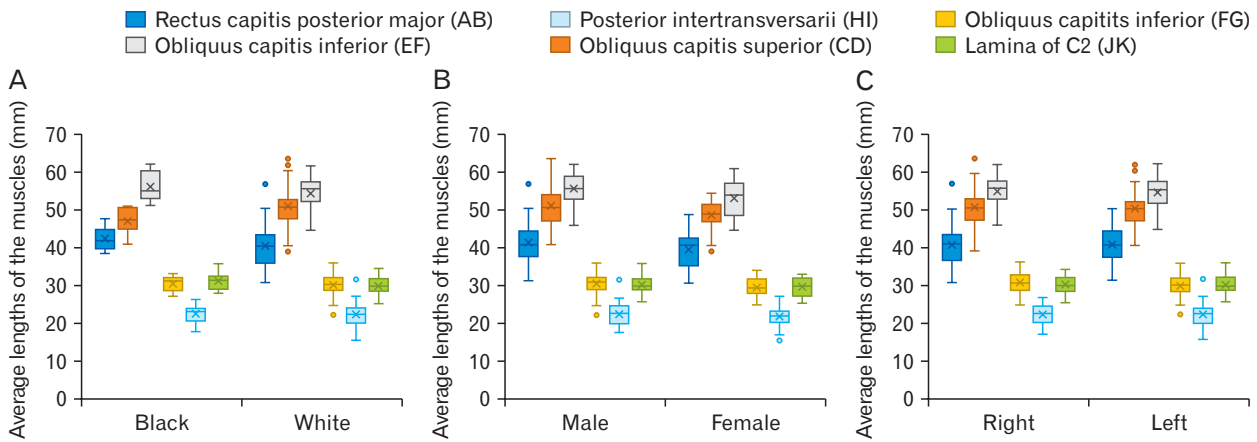
Fig. 4. Average lengths (mm) obtained of all the borders of the triangles. Comparing these measurements for the black- and white ancestry groups (A), females, males (B) as well as left- and right sides (C). Letters in brackets refer to the reference points inserted, and distance measured between the points.
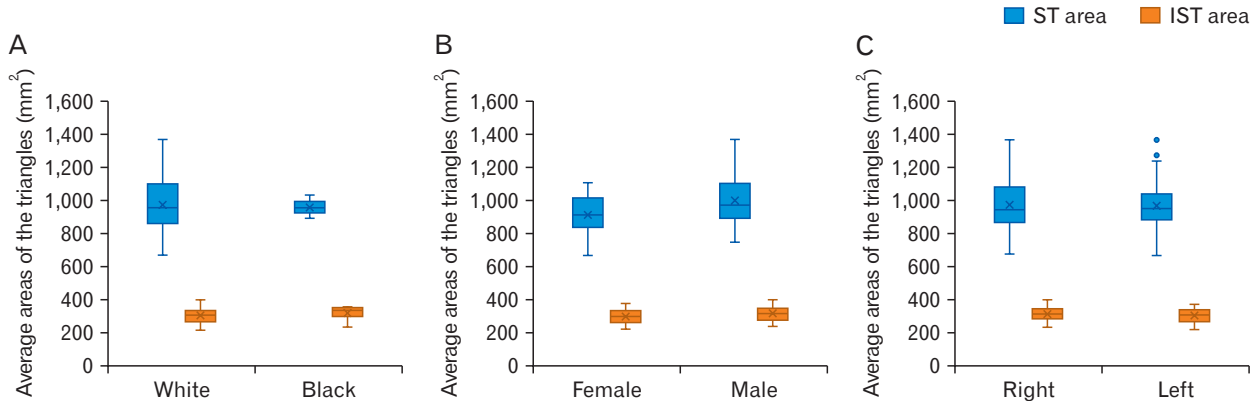

Fig. 5. Average areas (mm^2) obtained for the suboccipital triangle (ST) and the inferior suboccipital triangle (IST). Comparing these areas for the black- and white ancestry groups (A), females, males (B) as well as left- and right sides (C).

sistent. The data obtained for the areas of the triangles are illustrated in Fig. 5.

The vertebral artery was clearly visible and easily identifiable within the IST in 87.7% (57/65) fully dissected suboccipital regions. The term "easily identifiable" here does not mean that the artery is immediately and superficially visible within the IST. Rather it means that there was not a considerable amount of connective tissue and fat that had to be dissected out of the IST to visualize the artery when compared to the ST. In the remaining eight IST's, the VA could not be classified as "easily identifiable", as there was a substantial amount of connective tissue occluding the VA. In all dissected samples, a substantial layer of fatty connective tissue was observed to be both covering the ST, as well as within the triangle itself, surrounding the vertebral artery segment and its associated venous plexus. No accessory suboccipital muscles were observed in any triangles.

Inferential statistics was further conducted on the data collected to explore any possible relationships between the measurements taken and the side of body, sex and/or ancestry of the cadaver. Before any of these relationships were examined, a Shapiro–Wilk test was performed to test whether the data obtained in this study had a normal distribution. The results of this test are summarised in Table 3, which indicates that all the data obtained had a normal distribution with P-values larger than 0.05.

To evaluate the repeatability and reliability of the measurements taken, an ICC test was conducted. The measurements were repeated by the main author for ten cadavers (ICC-1 value) as well as by an independent researcher (ICC-2 value). All the ICC values obtained are summarised in Table 4.

Table 3. A table summarising the results of the Shapiro–Wilk test conducted to test whether the data obtained were normally distributed

Measurement	P-value
Length right rectus capitis posterior major (mm) [AB]	0.338
Length left rectus capitis posterior major (mm) [AB]	0.453
Length right OCS (mm) [CD]	0.616
Length left OCS (mm) [CD]	0.120
Length right OCI (mm) [EF]	0.227
Length left OCI (mm) [EF]	0.865
Length right OCI in IST (mm) [FG]	0.990
Length left OCI in IST (mm) [FG]	0.717
Length right posterior intertransversarii (mm) [HI]	0.458
Length left posterior intertransversarii (mm) [HI]	0.350
Length right lamina of C2 vertebra (mm) [JK]	0.594
Length left lamina of C2 vertebra (mm) [JK]	0.311
Area right ST (mm^2)	0.647
Area left ST (mm^2)	0.410
Area right IST (mm^2)	0.327
Area left IST (mm^2)	0.196

OCS, obliquus capitis superior; OCI, obliquus capitis inferior; ST, suboccipital triangle; IST, inferior suboccipital triangle. P-values larger than 0.05 indicates normal distributed data.

Table 4. A table summarising the results of the ICC test

Measurements	ICC value 1	ICC value 2
Length right rectus capitis posterior major (mm) [AB]	0.984	0.722
Length left rectus capitis posterior major (mm) [AB]	0.993	0.857
Length right OCS (mm) [CD]	0.862	0.954
Length left OCS (mm) [CD]	0.937	0.857
Length right OCI (mm) [EF]	0.904	0.981
Length left OCI (mm) [EF]	0.942	0.916
Length right OCI in IST (mm) [FG]	0.978	0.814
Length left OCI in IST (mm) [FG]	0.960	0.671
Length right posterior intertransversarii (mm) [HI]	0.975	0.774
Length left posterior intertransversarii (mm) [HI]	0.945	0.919
Length right lamina of C2 vertebra (mm) [JK]	0.922	0.721
Length left lamina of C2 vertebra (mm) [JK]	0.966	0.894
Area right ST (mm^2)	0.982	0.899
Area ST (mm^2)	0.990	0.952
Area right IST (mm^2)	0.943	0.548
Area left IST (mm^2)	0.945	0.806

ICC, intraclass correlation coefficient; OCS, obliquus capitis superior; OCI, obliquus capitis inferior; ST, suboccipital triangle; IST, inferior suboccipital triangle. ICC value 1 refers to the Intra-observer error while ICC value 2 to the Inter-observer error.

The measurements taken on the left side of the suboccipital region (for both triangles) was compared to those of the right side, by means of a paired sample *t*-test. A P-value of $P \leq 0.05$ was regarded as statistically significant. No statistically significant difference was noted between left and right sides for all the measurements, as indicated in Table 5. This means that the data can be combined for further statistical

Table 5. Table summarising results of the paired sample t-tests, comparing the left- and right sides' measurements

Measurements	P-value
Length rectus capitis posterior major [AB]	0.880
Length OCS [CD]	0.904
Length OCI [EF]	0.742
Length obliquus capitis inferior in IST [FG]	0.213
Length posterior intertransversarii [HI]	0.922
Length lamina [JK]	0.912
Area ST	0.990
Area IST	0.521

OCS, obliquus capitis superior; OCI, obliquus capitis inferior; IST, inferior suboccipital triangle; ST, suboccipital triangle. P-values larger than 0.05 indicates no statistically significant difference between the left- and right sides.

Table 6. A table summarizing the results from pearson chi-square tests investigating the measurements and their possible relationship to sex or ancestry of the cadavers

Measurement description	Sex P-value	Ancestry P-value
Length rectus capitis posterior major [AB]	0.418	0.418
Length OCS [CD]	0.418	0.418
Length OCI [EF]	0.418	0.418
Length OCI in IST [FG]	0.479	0.563
Length posterior intertransversarii [HI]	0.418	0.418
Length lamina [JK]	0.370	0.563
Area ST	0.418	0.418
Area IST	0.418	0.418

OCS, obliquus capitis superior; OCI, obliquus capitis inferior; IST, inferior suboccipital triangle; ST, suboccipital triangle. P-values larger than 0.05 indicates no statistically significant difference between the sex- and ancestry groups of the cadavers.

analysis.

The data was then reorganized into categories based on the sex and ancestry of the cadavers for further statistical analysis including chi-square tests. This is done to explore any possible relationship between the sex or ancestry of the cadaver to the measurements taken. Pearson's chi-square tests were conducted to compare the measurements taken to the sex and ancestry of the cadaver, respectively. No statistically significant difference was found for the measurements related to sex and/or ancestry of the cadavers, as summarised in Table 6.

Discussion

The ST is both an important anatomical- and surgical landmark that is most often used to identify and mobilize the third segment of the vertebral artery (V3) as it travels from

the transverse foramen of the C2 vertebra to the transverse foramen of the C1 vertebra in a medial to lateral direction [7]. However, often anomalous anatomy, scar tissue and lesions make the visualization of the ST and the vertebral artery running through it challenging. These pathologies and the consequent obscured anatomy increase the chances of iatrogenic vertebral artery injury. La Rocca et al. [9] has therefore defined a new IST that can be used to locate V3 more proximally. Regardless of whether the ST or the IST is used as the landmark to expose V3, understanding the anatomy of the suboccipital region, as well as the borders and relations of the two triangles is of vital importance before one can begin to locate the artery.

This study firstly examined the anatomy of ST which included the length of its muscular borders as well as the area of the triangle. The ST is bounded by three muscles including the RCPM superiorly with an average length of 40.78±5.60 mm, the OCS laterally with an average length of 51.23±5.04 mm and the OCI inferiorly with an average length of 54.83±4.44 mm. No statistically significant difference was found between the measurements and calculations when comparing the left and right sides (P-value=0.990). Furthermore, possible relationships between the measurements and/or calculations and the ancestry and sex of the cadaver was explored, and no statistically significant difference was noted (P-value=0.418 for both ancestry and sex). The mean area of the ST was approximately 969.82±133.15 mm^2.

A study conducted by Kalmanson et al. [16], measured the borders and area of the ST while the cervical spine was in a neutral position, and then again when the head was in a forward position. The length of the RCPM was published to be 48±8 mm, the length of OCS was published to be 52±5 mm, the length of OCI was published to be 49±4 mm, with the overall area of the ST being 1,040±190 mm^2 [16]. The measurements obtained by the current study found the average length of the RCPM and OCS muscles, as well as the area of the ST overall to be less than the values obtained by Kalmanson et al. [16], and the average length of the OCI to be longer. When considering the average standard deviation values of both sets of results however, it is evident that although the results are not a perfect match, they do in fact align with each other.

One obvious reason for the difference between the results recorded by this study, and those recorded by Kalmanson et al. [16] is the difference in the methodologies of data collection. Instead of measuring the lengths of the physical

muscles as this study did, Kalmanson et al. [16] dissected away the muscles and used CT scans to generate 3D models of each specimen, and then superimposed the muscles forming the ST onto the computer-generated model. This was achieved by estimating each muscle to be a straight line extending from the muscles' origin to insertion as defined in anatomic literature [16]. Additionally, the specimens in this study did not have their cervical spines intentionally spaced in a neutral position, and it is therefore entirely possible that some of the measurements were taken with the cervical spine slightly misaligned. It can also be noted here that the study performed by Kalmanson et al. [16] consisted of a relatively sample size of 13 cadavers.

Similarly, the anatomy of the IST was investigated by examining its muscular and bony borders and calculating its area. The IST is bounded by two muscles which include the posterior intertransversarii muscle laterally with an average length of 22.29±2.81 mm and a segment of the OCI muscle superiorly with an average length of 30.18±2.84 mm. The third border of this triangle is formed by the lamina of the C2 vertebra with an average length of 30.06±2.31 mm (these borders have been described in more details in the methodology of this study). No statistically significant difference was found when comparing the measurements and associated calculations between the left and right sides (P=0.521). Additionally, any possible relationships between the measurements and/or calculations and the ancestry and sex of the cadaver was investigated. No such relationships were found to exist as no statistically significant difference was noted (P-value=0.418 for both ancestry and sex).

This study obtained a mean area of the IST of 307.76± 41.32 mm^2. These measurements do not correlate to the study published by La Rocca et al. [9], which to the authors knowledge is currently the only additional piece of literature published on the IST. La Rocca et al. [9] found the mean area of the IST to be 187.1 mm^2 and did not distinguish between right and left sides [8]. This considerable difference in averages is a consequence of the difference in the definition and therefore the resulting measurements of the superior border of the IST. La Rocca et al. [9] defined the border simply as the length of OCI – although it is unclear if the entire border was in fact measured, whereas in this study the border was specified to be only the segment of the muscle between its insertion and the intersection of its inferior border with the superior border of the lamina of C2 vertebra. In keeping with this, as the defined length of the OCI muscle changed

between studies, so too would the angle between the muscle and the lamina of C2. Although La Rocca et al. [9] did not publish the values of their angles, nor the values of the length of their borders, it can consequently be inferred that as the angle between the OCI muscle and the lamina of C2 increases, the overall area of the IST would decrease. It is therefore possible that La Rocca et al. [9] assumed a more obtuse angle, and this therefore resulted in a smaller area. It is also prudent to note here that the method of area calculation could also contribute to the dissimilar average; although La Rocca et al. [9] did not state the method with which the area was calculated, while this study made use of Herons Formula. It can also be noted here that La Rocca and colleagues study consisted of a sample of five cadaveric specimens from an Italian population while this study's sample consisted of 33 cadavers, all from a South African population.

The value published by La Rocca et al. [9] for the average area of the IST (187.1 mm^2), is considerably smaller than the value published by Kalmanson et al. [16] for the average area of the ST (1,040 mm^2). This study too, found the average area of the ST to be significantly larger than the average area the IST (969.82 mm^2 vs. 307.76 mm^2, respectively). This is not only evident from the measurements of each triangles associated borders and the value of the area calculated, but also simply by visual inspection of the suboccipital region (please refer to Figs. 1, 3 for an illustration of the relative sizes of the triangles). Once again, this difference between previous studies results can be attributed to differing methodologies and borders.

The vertical segment of the third part of the vertebral artery (V3v) is located within the IST as it runs superolaterally between the transverse foramina of C2 and C1 vertebrae and is said to be slightly more superficial and therefore easier to locate and mobilize [9]. Additionally, the vertebral artery venous plexus was found to be less prominent at this level, which contributes to the ease of exposition. V3v, was found to be easily identifiable in in 87.69% of the sample. The term "easily identifiable" here does not mean that the artery is immediately and superficially visible within the IST. Rather it means that there was not a significant amount of connective tissue and fat and venous blood vessels that had to be dissected out of the IST to visualize the artery when compared to the ST. Additionally, the artery was observed to have a straightforward and predictable course within the IST, and could be located just medial to the posterior intertransversarii, as it runs superolateral from the transverse foramen of

C2 to the transverse foramen of C1 vertebra. No significant or occlusive venous plexuses were observed in this region. According to Muralimohan et al. [17], the VA has a noticeably tortuous and looping course in the region of the ST and is cushioned within a rich, sinus-like venous plexus. This venous plexus, as well as the depth of the artery within the ST and the dense layer of fibrous, fatty connective tissue located within the triangle, as well as between the triangle and the semispinalis capitis muscle that forms its roof, can make the location of the VA in the ST more challenging than in the IST. This dense layer of fibrous connective tissue and fat was easily observed during the dissection of all samples ST's and was found to be much more prominent at the level of the ST than of the IST. The data obtained by this study corresponds to the data obtained by La Rocca et al. [9], who also noted that at the level of the IST, the VA did not exhibit any significant looping or kinking, nor was it surrounded by any considerable periarterial venous plexuses.

The first and most obvious limitation of this study is the uneven distribution of the sex and ancestry of the cadavers available for this study. Double the number of cadaveric males (n=22) were available in comparison to females (n=11). Similarly, cadavers with European ancestry (n=28) were more readily available in comparison to cadavers of African ancestry (n=5).

Secondly, all dissections were performed with the cadavers in prone position. where the posterior side of the body is facing up, and the anterior side is facing down. Subsequently, the head and suboccipital region of the neck is fixed in a straight position, and this is not always the case during neurosurgical procedures. Had a far lateral approach been taken during dissections, measurements of the muscles involved in the rotation and lateral flexion of the head may have differed slightly.

In conclusion, both the ST and the IST can be used as reliable anatomical and surgical landmarks for the identification and exposition of the third segments of the VA. This study found the ST to have a significantly larger average area than the IST. Despite the IST being considerably smaller, location and exposition of V3v is more straightforward in the IST, compared to that of V3h within the ST. The IST an easily identifiable space that would for the exposure and control of the VA more proximally, when exposure of the distal aspect of the artery via the ST is not a viable option due to occlusion of the area by scar tissue or lesions. An accurate definition and understanding of the anatomy of the IST results in po-

tential clinical application of this space as a landmark with which to identify the third segment of the VA more proximally, should exposition of the artery within the ST not be a practical option. This is a key step in preventing iatrogenic vertebral artery injury (VAI), and the use of the IST in the prevention of VAI may be invaluable. The muscular and osseous borders of both triangles, as well as their average areas follow a normal and predictable distribution and have notably similar averages when comparing left and right sides of each triangle. Measurement and analysis of these borders and areas provided important anatomical information about the spaces and speak to the triangle's clinical relevance and importance as landmarks during posterior cervical spinal and cranio-cervical procedures.

ORCID

Kirsten Shannon Regan:
https://orcid.org/0000-0002-1247-1323
Gerda Venter: https://orcid.org/0000-0003-3471-4776

Author Contributions

Conceptualization: GV. Data acquisition: KSR. Data analysis or interpretation: KSR, GV. Drafting of the manuscript: KSR, GV. Critical revision of the manuscript: KSR, GV. Approval of the final version of the manuscript: all authors.

Conflicts of Interest

No potential conflict of interest relevant to this article was reported.

Funding

None.

Acknowledgements

References

1. Standring S. Gray's anatomy: the anatomical basis of clinical practice. 41st ed. Elsevier; 2016. p. 457-8, 744-5.
2. Kikuta S, Iwanaga J, Kusukawa J, Tubbs RS. Triangles of the neck: a review with clinical/surgical applications. Anat Cell Biol 2019;52:120-7.
3. Yamauchi M, Yamamoto M, Kitamura K, Morita S, Nagakura R, Matsunaga S, Abe S. Morphological classification and comparison of suboccipital muscle fiber characteristics. Anat Cell Biol 2017;50:247-54.
4. George T, Tadi P. Anatomy, head and neck, suboccipital muscles [Internet]. StatPearls; 2022 [cited 2022 Nov 25]. Available from: https://www.ncbi.nlm.nih.gov/books/NBK567762/
5. Sriamornrattanakul K, Akharathammachote N, Chonhenchob A, Mongkolratnan A, Niljianskul N, Phoominaonin IS, Ariyaprakai C, Wongsuriyanan S. Course of the V3 segment of the vertebral artery relative to the suboccipital triangle as an anatomical marker for a safe far lateral approach: a retrospective clinical study. Surg Neurol Int 2022;13:304.
6. Arnautović KI, Al-Mefty O. The microsurgical anatomy of the suboccipital vertebral artery and its surrounding structures. Oper Tech Neurosurg 2002;5:1-10.
7. Tjahjadi M, Rezai Jahromi B, Serrone J, Nurminen V, Choque-Velasquez J, Kivisaari R, Lehto H, Niemelä M, Hernesniemi J. Simple lateral suboccipital approach and modification for vertebral artery aneurysms: a study of 52 cases over 10 years. World Neurosurg 2017;108:336-46.
8. Fisahn C, Burgess B, Iwanaga J, Alonso F, Chapman JR, Oskouian RJ, Tubbs RS. A previously unreported arterial variant of the suboccipital region based on cadaveric dissection. J Neurol Surg Rep 2017;78:e40-2.
9. La Rocca G, Altieri R, Ricciardi L, Olivi A, Della Pepa GM. Anatomical study of occipital triangles: the 'inferior' suboccipital triangle, a useful vertebral artery landmark for safe postero-lateral skull base surgery. Acta Neurochir (Wien) 2017;159:1887-91.
10. Molinari RW, Chimenti PC, Molinari R Jr, Gruhn W. Vertebral artery injury during routine posterior cervical exposure: case reports and review of literature. Global Spine J 2015;5:528-32.
11. George B, Blanquet A, Alves O. The V3 segment of the vertebral artery: surgery around the craniocervical junction. Oper Tech Neurosurg 2002;5:50-74.
12. Khanfour AA, El Sekily NM. Relation of the vertebral artery segment from C1 to C2 vertebrae: an anatomical study. Alex J Med 2015;51:143-51.
13. Balik V, Takizawa K. Safe and bloodless exposure of the third segment of the vertebral artery: a step-by-step overview based on over 50 personal cases. Neurosurg Rev 2019;42:991-7.
14. Detton AJ. Grant's dissector. 16th ed. Wolters Kluwer; 2016. p. 16-7.
15. Lowry HV. Heron's formula. Math Gaz 1964;48:312-3.
16. Kalmanson OA, Khayatzadeh S, Germanwala A, Scott-Young

M, Havey RM, Voronov LI, Patwardhan AG. Anatomic considerations in headaches associated with cervical sagittal imbalance: a cadaveric biomechanical study. J Clin Neurosci 2019; 65:140-4.

17. Muralimohan S, Pande A, Vasudevan MC, Ramamurthi R. Suboccipital segment of the vertebral artery: a cadaveric study. Neurol India 2009;57:447-52.